



iMDA-BN: Identification of miRNA-disease associations based on the biological network and graph embedding algorithm



Kai Zheng^{a,1}, Zhu-Hong You^{b,1,*}, Lei Wang^{b,c,*}, Zhen-Hao Guo^b

^aSchool of Computer Science and Technology, China University of Mining and Technology, Xuzhou 221116, China

^bXinjiang Technical Institutes of Physics and Chemistry, Chinese Academy of Science, Urumqi 830011, China

^cCollege of Information Science and Engineering, Zaozhuang University, Zaozhuang 277100, China

ARTICLE INFO

Article history:

Received 4 July 2020

Received in revised form 24 August 2020

Accepted 26 August 2020

Available online 2 September 2020

Keywords:

miRNA

Disease

Heterogeneous information

The biological network

Graph embedding algorithm

ABSTRACT

Benefiting from advances in high-throughput experimental techniques, important regulatory roles of miRNAs, lncRNAs, and proteins, as well as biological property information, are gradually being complemented. As the key data support to promote biomedical research, domain knowledge such as intermolecular relationships that are increasingly revealed by molecular genome-wide analysis is often used to guide the discovery of potential associations. However, the method of performing network representation learning from the perspective of the global biological network is scarce. These methods cover a very limited type of molecular associations and are therefore not suitable for more comprehensive analysis of molecular network representation information. In this study, we propose a computational model based on the Biological network for predicting potential associations between miRNAs and diseases called iMDA-BN. The iMDA-BN has three significant advantages: I) It uses a new method to describe disease and miRNA characteristics which analyzes node representation information for disease and miRNA from the perspective of biological networks. II) It can predict unproven associations even if miRNAs and diseases do not appear in the biological network. III) Accurate description of miRNA characteristics from biological properties based on high-throughput sequence information. The iMDA-BN predictor achieves an AUC of 0.9145 and an accuracy of 84.49% on the miRNA-disease association baseline dataset, and it can also achieve an AUC of 0.8765 and an accuracy of 80.96% when predicting unknown diseases and miRNAs in the biological network. Compared to existing miRNA-disease association prediction methods, iMDA-BN has higher accuracy and the advantage of predicting unknown associations. In addition, 45, 49, and 49 of the top 50 miRNA-disease associations with the highest predicted scores were confirmed in the case studies, respectively.

© 2020 Published by Elsevier B.V. on behalf of Research Network of Computational and Structural Biotechnology. This is an open access article under the CC BY-NC-ND license (<http://creativecommons.org/licenses/by-nc-nd/4.0/>).

1. Introduction

MicroRNAs (miRNAs) are small, non-coding RNA molecules that affect basic biological processes by base pairing with targeted mRNAs [1,2]. In particular, many studies have revealed that miRNAs act as negative gene regulators in a variety of human diseases and are involved in disease processes such as breast cancer, myasthenia gravis, primary biliary cirrhosis, and the like [3–5]. This suggests that miRNAs can promote the development of new

therapeutic strategies by acting as biomarkers for certain diseases. Therefore, exploring how to predict the relationship between miRNA and disease on a large scale has always been a research hotspot in the field of bioinformatics.

In recent years, many predictive tools have been proposed that convert each node in the network (including miRNAs and diseases) into low-dimensional potential representations to calculate network representation associations in order to identify miRNA-diseases association in the context of known network structures. However, since most predictive tools only introduce intermediary to build a two-layer network (like the two-layer network composed of miRNA-disease association network, miRNA similarity network and disease similarity network), the amount of information represented by the network describing the nodes is relatively rare. For example, Shi *et al.* proposed a computational model for predicting potential miRNA-disease associations by integrating miRNA-target networks, gene-disease networks, and protein-protein

* Corresponding authors at: Xinjiang Technical Institutes of Physics and Chemistry, Chinese Academy of Science, Urumqi 830011, China and College of Information Science and Engineering, Zaozhuang University, Zaozhuang 277100, China (L. Wang).

E-mail addresses: zhuhongyou@ms.xjb.ac.cn (Z.-H. You), leiwang@ms.xjb.ac.cn (L. Wang).

¹ The authors wish it to be known that, in their opinion, the first two authors should be regarded as joint First Authors.

interaction networks. This method introduces many networks but does not quantify the network representation information of nodes from the entire network [6]. Similarly, Mork et al. constructed a miRNA-protein-disease network for association prediction which contributed greatly to inferring potential associations from the network structure but was still not comprehensive enough [7]. Later, Yang et al. calculated miRNA functional similarity by constructing a miRNA gene network to improve the performance of miRNA-disease association prediction. The contribution of this method to the field is obvious, but the constructed two-layer network does not truly reflect the relationship between nodes in reality [8]. In addition, Chen et al. proposed a prediction model based on binary network projection called BNPMDA, which introduces Medical Subject Headings to describe disease information [9]. Furthermore, there are many predictive tools that use domain knowledge as a supplement to high-throughput data to improve prediction accuracy, such as gene ontology (GO), medical subject terms, and miRNA-disease-associated network information [10–12]. For example, Lan et al. proposed a computational framework called KBMF-MDI, which uses miRNA sequence similarity to improve model performance [13]. Later, Wang et al. used natural language processing techniques to extract miRNA sequence features for the first time in the miRNA-disease association prediction model, which made an important contribution to accurately describe miRNA characteristics [14].

In this study, we propose a novel miRNA-disease association predictor based on biological networks and graph embedding algorithms to describe the characteristics of miRNAs and diseases from the perspective of complex biological network, called iMDA-BN. Different from the previous method, the new predictor has the following improvements: I) Biological networks composed of miRNA, lncRNA, protein, drug, and disease can describe the network representation of miRNAs and diseases from the perspective of the entire network, rather than being restricted to intermediaries. II) The association of pairs of new diseases and new miRNAs can be predicted and has a high degree of accuracy. III) Sequence information based on high-throughput sequencing is used to accurately quantify miRNA function information. In summary, the correlation of the three improvements is that they are all improvements made to improve the performance of the model and solve the defects of the existing methods. In iMDA-BN, 9 relationship types are integrated, including miRNA-lncRNA, miRNA-disease, miRNA-protein, lncRNA-disease, lncRNA-protein, protein-disease, drug-protein, drug-disease, protein-protein and 105,546 associations to build the biological network to assist in predicting potential associations between miRNA and disease. To our knowledge, this is the largest biological network for predicting miRNA-disease associations. To verify the performance of the iMDA-BN, we applied it to the benchmark data set to achieve an AUC of 0.9145 with an accuracy of 84.49%. And when predicting the associations between new diseases and new miRNAs, it can achieve an AUC of 0.8765 with an accuracy of 80.96%. In addition, in order to verify the robustness of the proposed predictor, three diseases were used for case studies. From the performance in various evaluations, the proposed prediction model based on Biological Network can be used as a good tool for predicting tasks.

2. Materials and methods

2.1. Data sets

2.1.1. The baseline data set of miRNA-disease association

With the deepening of biomedical research, the demand for integrated miRNA disease association databases is also growing, and various public databases and benchmark data sets have

emerged. They manually collected a large number of miRNA-disease association entries from the literature, for example, HMDD v3.0, dbDEM v2.0 and miR2Disease [15–17]. In this study, HMDD v3.0 was selected as the baseline database because it has the most comprehensive miRNA-disease association to date, collecting 32,281 experimentally supported miRNA-disease associations consisting of 1102 miRNA genes and 850 diseases. Due to the update of the version and the overlap of evidence supporting the association, they were combined into a group of associations covering 1206 miRNAs and 894 diseases. In this group, 901 miRNAs have sequence information in miRbase [18]. Therefore, the final data set included 16,427 associations consisting of 901 miRNAs and 877 diseases were used in our experiments.

2.1.2. The baseline data set of miRNA sequence information

With the development of high-throughput sequencing technology, biological characteristics such as miRNA sequence information have been gradually supplemented, and many public databases have begun to collect and integrate the biological information, including miRbase, PMRD and MicroRNAdb [19,20]. Among them, miRbase has the most complete miRNA information, containing 24,521 microRNA loci from 206, which can process 30,424 mature microRNA products. Therefore, in this experiment we downloaded high-throughput data from miRNAs from miRbase to complement miRNA sequence information. The database is accessible free of charge via the web server <http://www.mirbase.org/>.

2.1.3. The biological network

The complex homogeneous network constructed with associations between molecules can use the network representation information of its nodes as features to predict associations. The Biological Network consists of known molecules, as shown in Fig. 1. However, few predictors based on the entire molecular network to describe miRNA and disease characteristics have been proposed. The biological network (BN) constructed by Guo et al. provides a new perspective [21]. In order to fill this part of the research gap, we introduce the biological network (BN) into the prediction of miRNA-disease association. So far, the biological network consists of small biomolecule transcripts (proteins, lncRNAs and miRNAs), drugs and diseases. As shown in Table 1, there are nine kinds of associations which are miRNA-disease (MDA), miRNA-lncRNA (LMA), miRNA-protein (MPI), lncRNA-disease (LDA), lncRNA-protein (LPI), protein-disease (PDA), protein-protein (PPI), drug-protein (DPI), drug-disease (DDI).

Based on the above reference database, the number of various types of nodes in the statistical biological network is as shown in Table 2.

2.2. Methods

2.2.1. Attribute information of miRNAs and diseases

Semantic descriptor of disease: Disease descriptors describe disease attributes in medical subject vocabulary terms and organize them in Directed Acyclic Graphs (DAGs) where edges represent the association between diseases and nodes indicate disease. One of the core issues in the extraction of disease information is how to measure disease semantic relevance through the Medical Subject Headings (MeSH) terms [11]. In disease DAG, the association between the two diseases depends on their location/depth in the DAG, and if the two diseases have semantic similarities they will share more DAG parts. The semantic similarity $S_{sem}(d(i), d(j))$ of disease $d(i)$ and disease $d(j)$ are defined as follows:

$$S_{sem}(d(i), d(j)) = \frac{\sum_{k \in N_{d(i)} \cap N_{d(j)}} (C_{d(i)}(k) + C_{d(j)}(k))}{\sum_{k \in N_{d(i)}} C_{d(i)}(k) + \sum_{k \in N_{d(j)}} C_{d(j)}(k)} \quad (1)$$

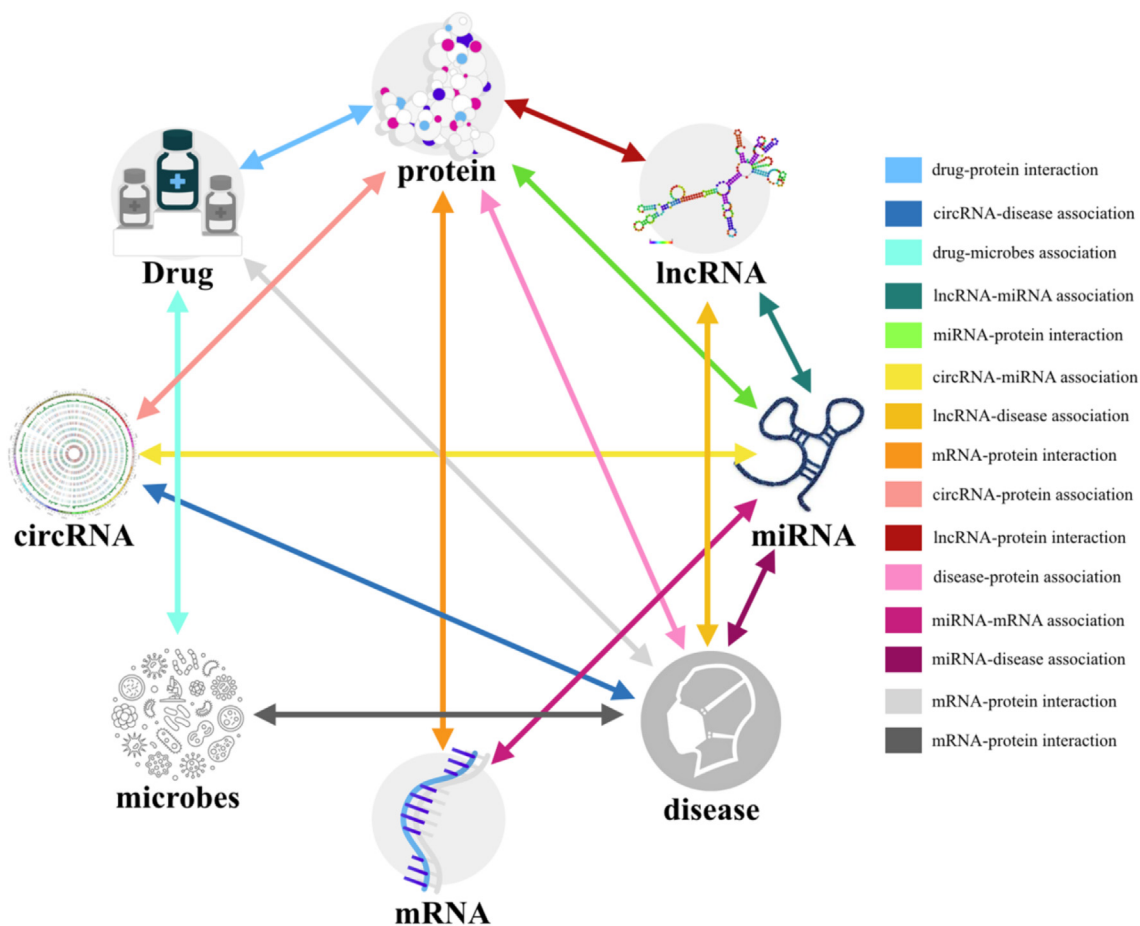


Fig. 1. The biological network.

Table 1
The nine associations that constitute the biological network.

Node	Association	Benchmark dataset	Version	Amount
miRNA	miRNA-disease	HMDD [15]	v3.0	16,427
	miRNA-lncRNA	lncRNASNP2 [33]	v1.0	8374
	miRNA-protein	miRTarBase [34]	v7.0	4944
lncRNA	lncRNA-disease	lncRNADisease [35]	v1.0	1264
		lncRNASNP2 [33]	v1.0	
	lncRNA-protein	lncRNA2Target [36]	v2.0	690
Protein	protein-disease	DisGeNET [37]	v6.0	25,087
	protein-protein	STRING [38]	v10.5	19,237
Drug	drug-protein	DrugBank [39]	v5.1	11,107
	drug-disease	CTD [40]	v2019	18,416
Total				105,546

Table 2
The number of five nodes in the biological network.

Node	MiRNA	lncRNA	Protein	Drug	Disease	Total
Amount	1023	769	1649	1025	2062	6528

$$\begin{cases} C_{d(i)}(k) = 1 & \text{if } k = d(i) \\ C_{d(i)}(k) = \max(\omega * C_{d(i)}(k') | k' \in \text{children of } k) & \text{if } k \neq d(i) \end{cases} \quad (2)$$

where $C_{d(i)}(k)$ is the semantic contribution of disease k to disease $d(i)$. ω is the contribution coefficient, which is set to 0.5 according

to the previous study [22]. $N_{d(i)}$ is a collection of all diseases that appear in the DAG of disease $d(i)$. When the semantic similarity between all diseases in the biological network is calculated, the semantic similarity matrix S_{sem} whose size is 2062×2062 can be obtained. Therefore, according to previous studies [14,23–25], the descriptor for disease $d(i)$ can be defined as follows:

$$attribute(d(i)) = S_{sem}(d(i)) \tag{3}$$

where $S_{sem}(d(i))$ is a vector consisting of a collection of semantic similarities between disease $d(i)$ and all diseases. Descriptors corresponding to 877 diseases in HMDD v3.0 were used to construct attribute information of the disease.

Sequence descriptor of miRNA: The properties of the miRNA are represented by sequence information. For the sake of simplicity, k -mer is used to convert the sequence into a numerical vector, where k represents the length of the segmented subsequence [26]. For example, the 3-mer miRNA sequence can be expressed as AAA, UAA, ... UUU, and the number of all combinations is $4*4*4 = 64$. Due to the short miRNA sequence, the feature vector composed of 4-mer and 5-mer algorithm has a large number of features that are 0, which makes the feature vector noise. In this experiment, we use 3-mer to segment the sequence and use the normalized frequency of 64 subsequences as the sequence descriptor $attribute(m(j))$ where $m(j)$ is the j th miRNA.

2.2.2. Node representation

In order to effectively represent the relationship between each node and other nodes in the entire biological network, a network embedding method named Node2Vec is utilized in this study [27]. Node2Vec method is based on the sampling node neighborhood strategy of random walk, and optimizes the neighborhood preserving likelihood objective by the Skip-gram model to obtain the network embedded representation of the node. The method simulates a random walk of each node, wherein the i -th node $c(i)$ in the walk can be described as follows:

$$P(c(i) = x | c(i-1) = v) = \begin{cases} \frac{\pi_{v,x}}{Z} & \text{if } v, x \in E \\ 0 & \text{otherwise} \end{cases} \tag{4}$$

where Z is the normalization constant and $\pi_{v,x}$ is defined as the unstandardized transition probability of nodes v and x :

$$\pi_{v,x} = \alpha_{pq}(t, x) * \omega_{v,x} \tag{5}$$

where $\omega_{v,x}$ is the weight of the edges v and x , and the unweighted graph used in this experiment is set to 1. $\alpha_{pq}(t, x)$ is used to adjust the search process, interpolating between BFS and DFS. It is defined as follows:

$$\alpha_{pq}(t, x) = \begin{cases} \frac{1}{p} & \text{if } d_{tx} = 0 \\ 1 & \text{if } d_{tx} = 1 \\ \frac{1}{q} & \text{if } d_{tx} = 2 \end{cases} \tag{6}$$

where d_{tx} is the shortest distance between node t and node x . p and q are the return parameter and the In-out parameter, respectively. And, the default parameters are used in this experiment. The specific details are shown in Fig. 2. By learning the low-dimensional potential representation of nodes in the entire biological network, each node can describe its network relationship through a 64-dimensional vector $manner(node(i))$. $node(i)$ is the i -th node in the network.

2.2.3. Stacked autoencoder

Information from multiple sources is integrated in the proposed model, including information on the characteristics of diseases and miRNAs, as well as network representations of diseases and miRNAs. This operation allows the feature to contain more information, however, due to the different scope and size of the data from different sources, the model will be overly complex and prone to overfitting. Therefore, stacked Autoencoder is adopted to obtain the appropriate subspace from the original feature space, which can express the main features of the high-dimensional vectors in a low-dimensional way. The encoder that encodes the input X as a hidden representation Y is defined as follows:

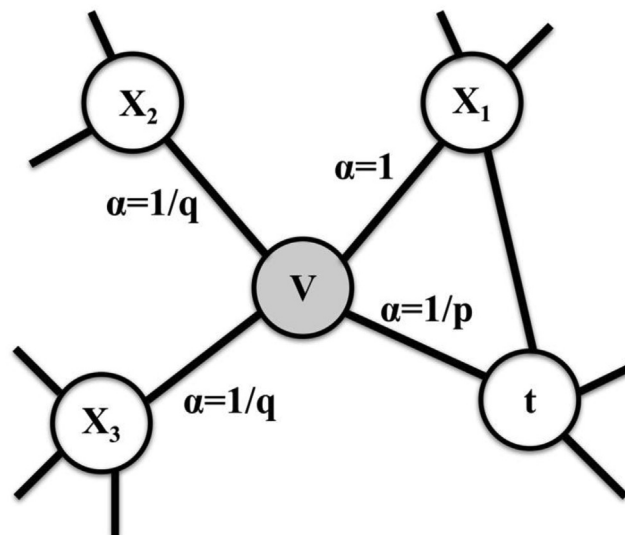


Fig. 2. The 2nd-order biased random walks procedure in Node2Vec.

$$Y = f(X) = S_c(W_1^T X + b_1) \tag{7}$$

The decoder that maps the hidden representation Y to the approximate output Z is defined as follows:

$$Z = g(Y) = S_d(W_2^T Y + b_2) \tag{8}$$

where S_c and S_d are the activation functions. W_1 and W_2 are relational parameters. b_1 and b_2 are bias parameters.

$$S_c(t) = S_d(t) = \max(0, Wt + b) \tag{9}$$

The principle of the autoencoder described above, and the stacked autoencoder used in this article is composed of multiple basic autoencoders. Specifically, we use disease semantic information as input X to train the first hidden layer to obtain the main features. Then train the second hidden layer through the main features to obtain more abstract deep features. Iterate back and forth until the final feature vector is obtained in the middle-hidden layer. In the experiment, keras framework is used, where the loss function is the mean-square error (MSE), the activation function is relu, and the optimization function is the Adam algorithm. The parameters used in the relevant models are all defaults.

2.2.4. Method overview

In this study, a new predictor called iMDA-BN was constructed to predict potential associations between miRNAs and diseases. The iMDA-BN is roughly divided into three parts, as shown in Fig. 3. Firstly, node attribute, miRNA-based high-throughput data information and disease semantic information are used to construct miRNA sequence descriptors and disease semantic descriptors, respectively. Secondly, edge embedding, the network representation learning based on Biological Network calculates the node representation of each miRNA and disease. Thirdly, the autoencoder is used to extract the deep features of disease semantic descriptors. Finally, training random forest models to calculate miRNA-disease association scores. Next, the details in the experiment are described in detail.

The choice of positive and negative samples: Specifically, the 16,427 miRNA-disease associations provided in HMDD are utilized as positive samples. The downsampling method was used to construct negative samples by randomly extracting the same number of associations from positive samples from 773,750 unconfirmed miRNA-disease associations. Although there may be potential

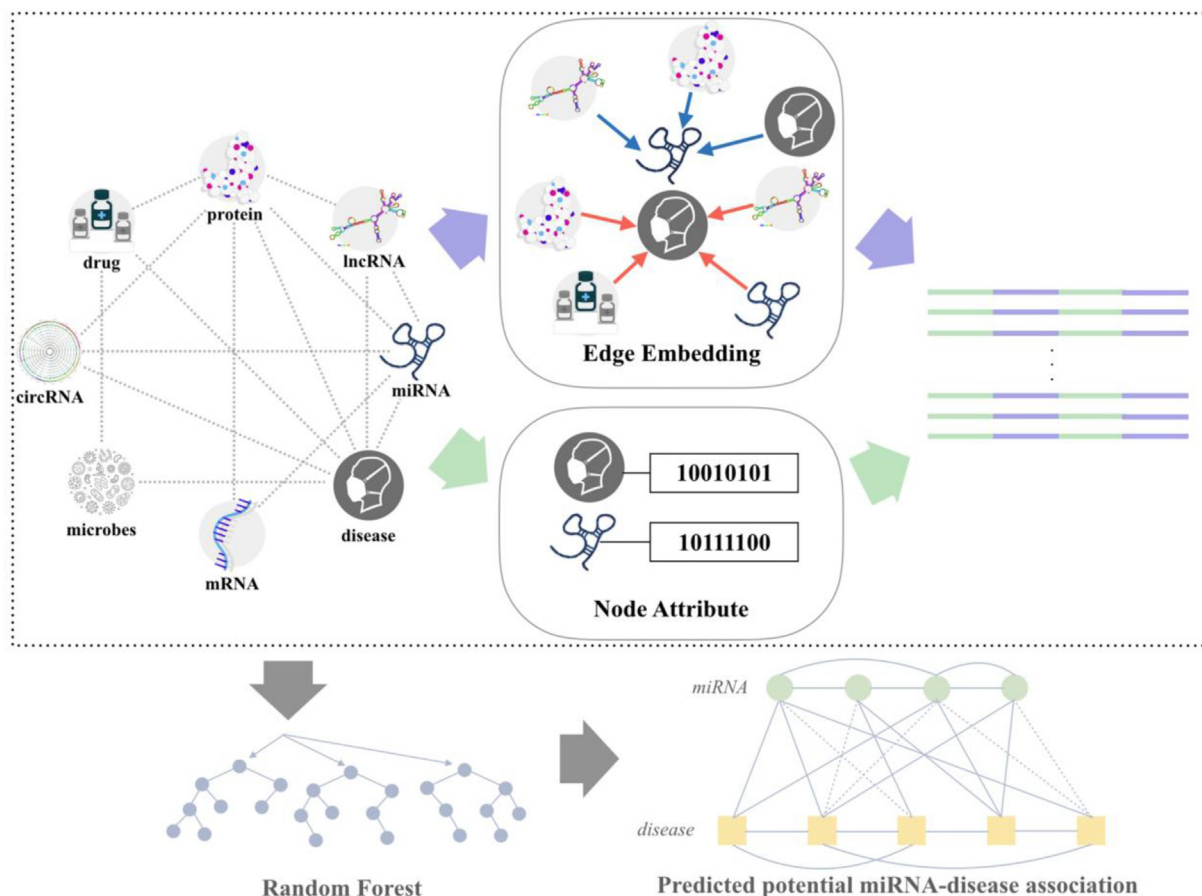


Fig. 3. The framework of iMDA-BN.

associations, the number of negative samples we selected was only $16427A \cdot (901 \times 877) \approx 2.08\%$ of the total number of samples. Therefore, there is a low probability of potential associations that can be ignored.

The construction of the final feature descriptor: As shown in Fig. 3, the final feature descriptor of size 256×32854 is represented by the miRNA sequence descriptor, the miRNA node, the disease semantic descriptor and the disease node representation. The final association descriptor F of disease $d(j)$ and miRNA $m(i)$ can be described as a 256-dimensional vector:

$$F(m(i), d(j)) = (\text{descriptor}(m(i)), \text{manner}(m(i)), \text{descriptor}(d(j)), \text{manner}(d(j))) \tag{10}$$

Prediction of miRNA-disease association by Random Forest: The final descriptor is used to train the random forest model and predict potential associations based on the trained model. In particular, the higher the prediction score, the more likely it is to be the candidate for potential associations. The parameters used in the relevant models are all defaults.

3. Experimental results

3.1. Performance of the new prediction method

In order to comprehensively evaluate the robustness and effectiveness of the iMDA-BN predictor, a 5-fold cross-validation was performed on the proposed model on the HMDD v3.0 dataset. It is divided into three steps: 1) The 32,854 associations used in this experiment were divided into five approximately equal and

disjoint subsets (The positive and negative samples in each subset are 1:1). 2) One of the subsets was selected as the test set to test the model performance, and the remaining four subsets were used as the training set to train model. 3) Repeat step 2 until that all subsets are selected as test sets. Thus, five sets of experimental results were obtained, and we reported them in Table 3 and Fig. 4, respectively. The area under the curve (AUC) is the area of the graph surrounded by the receiver operating characteristic curve (ROC) where the ROC is an evaluation criterion. It can be seen from Table 3 that the average AUC of the iMDA-BN has reached 0.9145, and the standard deviation is only 0.32%, which indicates that the proposed predictor is robust. In addition, the accuracy (Acc.), sensitivity (Sen.), precision (Prec.), specificity (Spec.), Matthews correlation coefficient (MCC) and the area under precision-recall (AUPR) of the proposed model are 84.49%, 84.20%, 84.79%, 84.70%, 68.99% and 91.92%. From the results of this part of the experiment (Table 3, Fig. 4 and Fig. 5), the method we proposed is discriminative.

3.2. Compare different strategies to generate feature descriptors

Real-world networks, such as the biological network, are composed of nodes and edges, each associated with an essential attribute. In this method, the proposed feature descriptor $F(m(i), d(j))$ is composed of the node attribute information *descriptor* and the node representation information *manner* that retains network structure information. In order to verify the reliability of the descriptors, we compare the three methods we implemented ourselves, using different descriptors in this experiment. Details are as follows.

Table 3
The result of 5-fold cross-validation of iMDA-BN on the HMDD v3.0 data set.

Test set	Acc. (%)	Sen. (%)	Prec. (%)	Spec. (%)	MCC (%)	AUC	AUPR
1	84.14	83.84	84.45	84.35	68.29	0.9100	0.9148
2	84.57	84.51	84.63	84.61	69.14	0.9133	0.9168
3	85.04	85.39	84.69	84.8	70.09	0.9185	0.9216
4	84.57	84.02	85.12	84.95	69.15	0.9159	0.9214
5	84.15	83.25	85.04	84.77	68.3	0.9150	0.9218
Average	84.49 ± 0.37	84.20 ± 0.80	84.79 ± 0.28	84.70 ± 0.23	68.99 ± 0.75	0.9145 ± 0.0032	0.9192 ± 0.0032

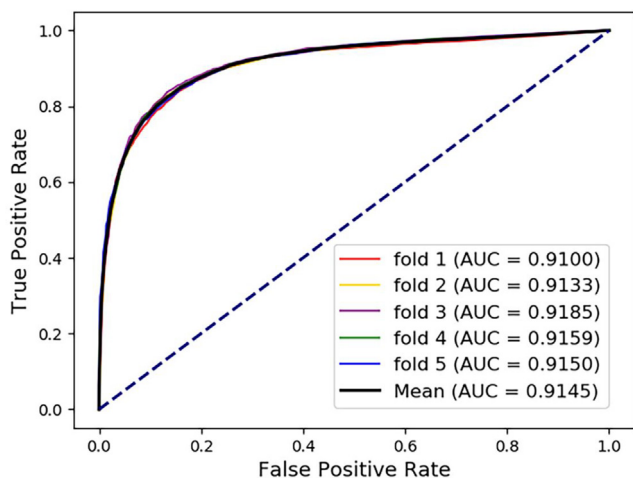


Fig. 4. ROC curves performed by iMDA-BN.

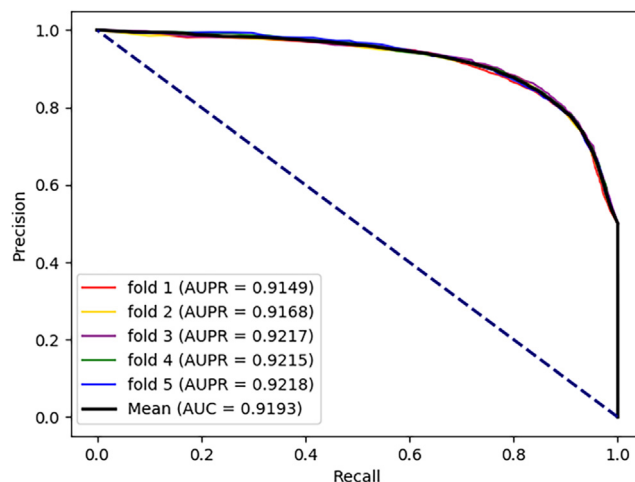


Fig. 5. PR curves performed by iMDA-BN.

- Descriptor “iMDA-BN (attribute)”: It consists of disease and miRNA attribute information, which can be described as $F_{attribute}(m(i), d(j)) = attribute(m(i), d(j))$.
- Descriptor “iMDA-BN (manner)”: It consists of disease and miRNA node representation information, which can be described as $F_{manner}(m(i), d(j)) = (manner(m(i)), manner(d(j)))$.
- Descriptor “iMDA-BN”: The proposed feature descriptor $F(m(i), d(j))$.

The above three descriptors all utilize the same random forest classifier, Medical Subject Headings and miRNA sequence information. Table 4 shows the scores of the three descriptors in the seven evaluation criteria including accuracy (Acc.), sensitivity (Sen.), specificity (Spec.), precision (Prec.) and Matthews correlation coefficient (MCC), AUC and AUPR. It can be seen that iMDA-BN outperforms other descriptors in the seven evaluation indicators, especially the AUC and MCC that measure the overall performance of the model. This suggests that multi-source knowledge that combines miRNA and disease attribute information with its node representation information in the network can describe the association between miRNA and disease from a more macro perspective, thereby characterizing the deeper meaning of multi-source data.

Furthermore, for miRNAs and diseases that are not in the network, their characteristics can be characterized by combining their attribute information and setting the manner part to 0. The performance of iMDA-BN (attribute) is verified in Fig. 6, indicating that the attribute information has considerable recognition. Therefore, in this way, we solve the problem of association prediction between miRNAs and diseases that are not in the network.

Table 4
The comparison of different types of feature descriptors.

Metric	Descriptor comparison		
	iMDA-BN (Attribute)	iMDA-BN (Manner)	iMDA-BN
Acc. (%)	80.96 ± 0.53	84.12 ± 0.28	84.49 ± 0.37
Sen. (%)	83.79 ± 1.12	83.85 ± 0.79	84.20 ± 0.80
Prec. (%)	78.14 ± 0.35	84.40 ± 0.29	84.79 ± 0.28
Spec. (%)	79.30 ± 0.28	84.31 ± 0.15	84.70 ± 0.23
MCC (%)	62.02 ± 1.11	68.25 ± 0.56	68.99 ± 0.75
AUC	0.8765 ± 0.0039	0.9106 ± 0.0034	0.9145 ± 0.0032
AUPR	0.8719 ± 0.0036	0.9143 ± 0.0031	0.9188 ± 0.0030

3.3. Comparison with highly related methods

In recent years, many predictors have been proposed for the potential association between miRNAs and diseases. We compare the performance of the iMDA-BN with 7 state-of-the-art methods, including Shi’s, BNPMDA, LMTRDA, HGIMDA, BRWHNHA, KBMF-MDI and KBMF-MDI. Table 5 not only lists the performance of the various methods, but also shows the prior knowledge of building the associated network and the attribute information of the nodes. From the results, the iMDA-BN is superior to other methods using less than four associations on AUC and is 4.9% higher than the average. It is shown that the node representation information based on the biological network can improve the effect of predicting associations between miRNA and disease. In addition, the proposed method has an improvement of 2.48% and 15.65% in performance compared to methods that do not use attribute information such as MDA-CNN and Shi’s, which means that attribute information can also improve prediction performance. Furthermore, in Table 5, a protein–protein interaction (PPI) network of human genes was used as a gene net-

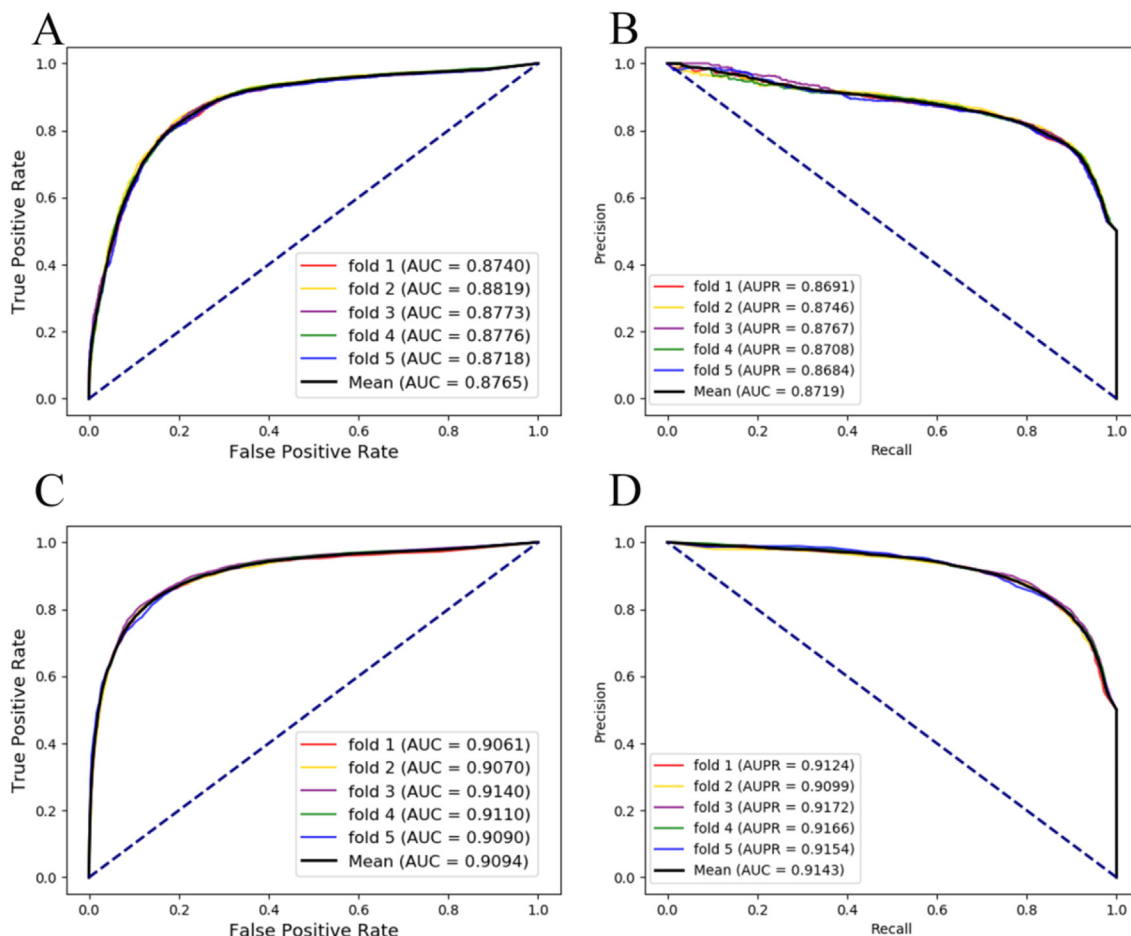


Fig. 6. ROC and PR curves performed by iMDA-BN (Attribute) and iMDA-BN (manner). (A) ROC curves performed by iMDA-BN (Attribute). (B) PR curves performed by iMDA-BN (Attribute). (C) ROC curves performed by iMDA-BN (manner). (D) PR curves performed by iMDA-BN (manner).

Table 5
The comparison with related models.

Association	Methods	Attribute	AUC scores	MDA samples
PPI, MPI, DPI	Shi's ¹	N/A	0.7580	518
	MDA-CNN ²	N/A	0.8897	2449
MDA	BNPMDA ³	MeSH	0.8980	5430
	LMTRDA ⁴	miRNA sequence, MeSH	0.9054	32,226
	HGIMDA ⁵	MeSH	0.8781	5430
	BRWHNHA ⁶	MeSH	0.8570	5430
MDA, DPI	KBMF-MDI ⁷	miRNA sequence, MeSH,	0.8725	6084
MDA, LDA, PPI, LMA, LPI, DPI, MPI, PDI, DDI	iMDA-BN	miRNA sequence, MeSH	0.9145	16,427

¹ This method is reported in [6].
² This method is reported in [23].
³ This method is reported in [9].
⁴ This method is reported in [14].
⁵ This method is reported in [41].
⁶ This method is reported in [42].
⁷ This method is reported in [13].

work, as in previous studies, since miRNAs affect disease by regulating gene expression post-transcriptionally [23].

3.4. Case study

In this part of the experiment, the iMDA-BN's the ability of predicting disease-associated miRNAs was validated by case studies of three common human diseases, assuming that prior knowledge are

only associations in HMDD v3.0. Specifically, the training set is made up of all the associations in the final descriptor. At the same time, we used the associations that did not appear in HMDD for the three diseases as a test set. After iMDA-BN gave prediction scores to the test set, the top 50 miRNAs with the highest score for each disease were validated in the dbDEMOC database and the miR2Di-sease database [16,17]. Breast cancer is the most common female cancer in developed countries [28]. Its incidence increases rapidly

Table 6
Prediction of the top 50 predicted miRNAs associated with breast neoplasms.

miRNA	dbDEMC	miR2D	miRNA	dbDEMC	miR2D
hsa-mir-181d-5p	confirmed	unconfirmed	hsa-mir-508-5p	confirmed	unconfirmed
hsa-mir-99b-5p	confirmed	unconfirmed	hsa-mir-154-5p	confirmed	unconfirmed
hsa-mir-330-5p	confirmed	unconfirmed	hsa-mir-581	confirmed	unconfirmed
hsa-mir-28-5p	confirmed	unconfirmed	hsa-mir-501-5p	confirmed	unconfirmed
hsa-mir-361-5p	confirmed	unconfirmed	hsa-mir-323a-5p	confirmed	unconfirmed
hsa-mir-371a-5p	confirmed	unconfirmed	hsa-mir-628-5p	confirmed	unconfirmed
hsa-mir-885-5p	confirmed	unconfirmed	hsa-mir-612	unconfirmed	unconfirmed
hsa-mir-455-5p	confirmed	unconfirmed	hsa-mir-490-5p	confirmed	unconfirmed
hsa-mir-651-5p	confirmed	unconfirmed	hsa-mir-188-5p	confirmed	unconfirmed
hsa-mir-1271-5p	confirmed	unconfirmed	hsa-mir-1299	confirmed	unconfirmed
hsa-mir-504-5p	confirmed	unconfirmed	hsa-mir-95-5p	confirmed	unconfirmed
hsa-mir-876-5p	confirmed	unconfirmed	hsa-mir-1296-5p	confirmed	unconfirmed
hsa-mir-454-5p	confirmed	unconfirmed	hsa-mir-582-5p	confirmed	unconfirmed
hsa-mir-532-5p	confirmed	unconfirmed	hsa-mir-512-5p	confirmed	unconfirmed
hsa-mir-1297	confirmed	unconfirmed	hsa-mir-1303	confirmed	unconfirmed
hsa-mir-449b-5p	confirmed	unconfirmed	hsa-mir-323b-5p	confirmed	unconfirmed
hsa-mir-433-5p	confirmed	unconfirmed	hsa-mir-889-5p	confirmed	unconfirmed
hsa-mir-544a	confirmed	unconfirmed	hsa-mir-1184	confirmed	unconfirmed
hsa-mir-136-5p	confirmed	confirmed	hsa-mir-500a-5p	confirmed	unconfirmed
hsa-mir-23c	unconfirmed	unconfirmed	hsa-mir-217-5p	confirmed	unconfirmed
hsa-mir-761	unconfirmed	unconfirmed	hsa-mir-518e-5p	confirmed	unconfirmed
hsa-mir-4500	unconfirmed	unconfirmed	hsa-mir-376b-5p	confirmed	unconfirmed
hsa-mir-346	confirmed	unconfirmed	hsa-mir-186-5p	confirmed	unconfirmed
hsa-mir-216a-5p	confirmed	unconfirmed	hsa-mir-498-5p	confirmed	unconfirmed
hsa-mir-382-5p	confirmed	unconfirmed	hsa-mir-764	unconfirmed	unconfirmed

Table 7
Prediction of the top 50 predicted miRNAs associated with Colon Neoplasms.

miRNA	dbDEMC	miR2D	miRNA	dbDEMC	miR2D
hsa-mir-16-5p	confirmed	unconfirmed	hsa-mir-505-5p	confirmed	unconfirmed
hsa-mir-29c-5p	confirmed	unconfirmed	hsa-mir-495-5p	confirmed	unconfirmed
hsa-mir-423-5p	confirmed	unconfirmed	hsa-mir-122-5p	confirmed	unconfirmed
hsa-mir-146b-5p	confirmed	unconfirmed	hsa-mir-34b-5p	confirmed	confirmed
hsa-mir-193a-5p	confirmed	unconfirmed	hsa-mir-7-5p	confirmed	confirmed
hsa-mir-98-5p	confirmed	unconfirmed	hsa-mir-370-5p	confirmed	unconfirmed
hsa-mir-124-5p	confirmed	confirmed	hsa-mir-34c-5p	confirmed	confirmed
hsa-mir-9-5p	confirmed	confirmed	hsa-mir-134-5p	confirmed	unconfirmed
hsa-mir-130b-5p	confirmed	confirmed	hsa-mir-491-5p	confirmed	unconfirmed
hsa-mir-128-3p	confirmed	confirmed	hsa-mir-212-5p	confirmed	unconfirmed
hsa-mir-199a-5p	confirmed	unconfirmed	hsa-mir-149-5p	confirmed	unconfirmed
hsa-mir-362-5p	unconfirmed	unconfirmed	hsa-mir-129-5p	confirmed	confirmed
hsa-mir-372-5p	confirmed	confirmed	hsa-mir-181a-2-3p	confirmed	confirmed
hsa-mir-27b-5p	confirmed	confirmed	hsa-mir-99b-5p	confirmed	unconfirmed
hsa-mir-494-5p	confirmed	unconfirmed	hsa-mir-144-5p	confirmed	unconfirmed
hsa-mir-139-5p	confirmed	confirmed	hsa-mir-182-5p	confirmed	confirmed
hsa-mir-92b-5p	confirmed	unconfirmed	hsa-mir-99a-5p	confirmed	unconfirmed
hsa-mir-10a-5p	confirmed	confirmed	hsa-mir-373-5p	confirmed	unconfirmed
hsa-mir-92a-2-5p	confirmed	unconfirmed	hsa-mir-29b-2-5p	confirmed	confirmed
hsa-mir-199b-5p	confirmed	unconfirmed	hsa-mir-20b-5p	confirmed	unconfirmed
hsa-mir-214-5p	confirmed	unconfirmed	hsa-mir-320a-5p	confirmed	unconfirmed
hsa-mir-217-5p	confirmed	unconfirmed	hsa-mir-28-5p	confirmed	unconfirmed
hsa-mir-590-5p	confirmed	unconfirmed	hsa-mir-26a-2-3p	confirmed	confirmed
hsa-mir-342-5p	confirmed	confirmed	hsa-mir-100-5p	confirmed	unconfirmed
hsa-mir-421	confirmed	unconfirmed	hsa-mir-302c-5p	confirmed	unconfirmed

with age, but its incidence decreases near the age of menopause [28]. Since some of the pathogenic factors of breast cancer are endogenous, this makes prevention very difficult. Recent studies have shown that mir-125b, mir-145, mir-21 and mir-155 in breast cancer tissues are significantly dysregulated compared to normal breast tissue [29]. In Table 6, we predicted potential breast neoplasms-associated miRNAs and verified the top 50 miRNAs with the highest scores, 45 of these miRNA-disease associations were confirmed. Colon cancer is the second most common cancer [30]. Since some colon cancer cells still cannot be eradicated by existing therapies, the study of the pathogenic principle has been

a hotspot in biomedical research [30]. Studies have shown that the promoters of hsa-miR-9, hsa-miR-129 and hsa-miR-137 are abnormally hypermethylated in colon cancer cells [31]. In Table 7, we predicted potential Colon Neoplasms-associated miRNAs and verified the top 50 miRNAs with the highest scores, of which 49 miRNA-disease associations were confirmed. Lymphoma is a blood cancer that develops from lymphocytes and originates from lymphocytes [32]. In Table 8, we predicted potential Lymphoma-associated miRNAs and verified the top 50 miRNAs with the highest scores, 49 of these miRNA-disease associations were confirmed.

Table 8
Prediction of the top 50 predicted miRNAs associated with Lymphomas.

miRNA	dbDEMC	miR2D	miRNA	dbDEMC	miR2D
hsa-mir-145-5p	confirmed	confirmed	hsa-mir-876-5p	confirmed	unconfirmed
hsa-let-7b-5p	confirmed	unconfirmed	hsa-let-7e-5p	confirmed	confirmed
hsa-let-7a-5p	confirmed	confirmed	hsa-mir-15b-5p	confirmed	unconfirmed
hsa-mir-182-5p	confirmed	unconfirmed	hsa-mir-199b-5p	confirmed	unconfirmed
hsa-mir-34a-5p	confirmed	unconfirmed	hsa-mir-106b-5p	confirmed	unconfirmed
hsa-mir-107	confirmed	unconfirmed	hsa-mir-192-5p	confirmed	unconfirmed
hsa-mir-424-5p	confirmed	unconfirmed	hsa-mir-106a-5p	confirmed	confirmed
hsa-mir-98-5p	confirmed	unconfirmed	hsa-mir-146b-5p	confirmed	unconfirmed
hsa-mir-195-5p	confirmed	unconfirmed	hsa-mir-33b-5p	confirmed	unconfirmed
hsa-mir-181b-5p	confirmed	unconfirmed	hsa-mir-196a-5p	confirmed	confirmed
hsa-mir-9-5p	confirmed	confirmed	hsa-mir-33a-5p	confirmed	unconfirmed
hsa-mir-218-5p	confirmed	unconfirmed	hsa-mir-125b-1-3p	unconfirmed	unconfirmed
hsa-mir-335-5p	confirmed	unconfirmed	hsa-mir-181d-5p	confirmed	unconfirmed
hsa-mir-196b-5p	confirmed	unconfirmed	hsa-mir-346	confirmed	unconfirmed
hsa-mir-138-5p	confirmed	unconfirmed	hsa-mir-100-5p	confirmed	unconfirmed
hsa-mir-29a-5p	confirmed	unconfirmed	hsa-mir-590-5p	confirmed	unconfirmed
hsa-let-7g-5p	confirmed	unconfirmed	hsa-mir-361-5p	confirmed	unconfirmed
hsa-mir-30b-5p	confirmed	confirmed	hsa-mir-421	confirmed	unconfirmed
hsa-mir-503-5p	confirmed	unconfirmed	hsa-mir-320b	confirmed	unconfirmed
hsa-mir-24-3p	confirmed	unconfirmed	hsa-mir-7-5p	confirmed	unconfirmed
hsa-mir-125b-5p	confirmed	unconfirmed	hsa-mir-149-5p	confirmed	confirmed
hsa-mir-374a-5p	confirmed	unconfirmed	hsa-mir-32-5p	confirmed	unconfirmed
hsa-mir-326	confirmed	unconfirmed	hsa-mir-216b-5p	confirmed	unconfirmed
hsa-mir-134-5p	confirmed	unconfirmed	hsa-mir-129-5p	confirmed	unconfirmed
hsa-mir-136-5p	confirmed	unconfirmed	hsa-let-7i-5p	confirmed	unconfirmed

4. Conclusion

With the development of bioinformatics, more and more predictors of potential associations have been proposed, and these methods have greatly promoted the development of biomedicine. However, they focus only on the association network of research content, and methods based on the entire biological network are scarce. Therefore, it is necessary to develop a biological network-based computational method to identify the association between potential miRNAs and diseases. In this paper, we propose a novel computational method based on a complex biological network composed of nine associations called iMDA-BN to predict the potential association between potential miRNAs and disease. From the experimental results, it is better than other most advanced methods, and it can predict the association between miRNA and disease that does not exist in the network. In addition, we also demonstrated the excellent ability of iMDA-BN to predict potential associations through three case studies, and achieved 90%, 98% and 98% accuracy. The reliability of iMDA-BN can be achieved mainly for three reasons: I) It uses a new method to describe disease and miRNA characteristics which analyzes node representation information for disease and miRNA from the perspective of biological networks. II) Accurate description of miRNA characteristics from biological properties based on high-throughput sequence information. III) It can predict unproven associations even if miRNAs and diseases do not appear in the biological network.

CRediT authorship contribution statement

Kai Zheng: Writing - original draft, Resources. **Zhu-Hong You:** Conceptualization, Methodology. **Lei Wang:** Writing - review & editing, Investigation, Supervision. **Zhen-Hao Guo:** Data curation, Software.

Declaration of Competing Interest

The authors declare that they have no known competing financial interests or personal relationships that could have appeared to influence the work reported in this paper.

Acknowledgements

This work is supported in part by Awardee of the NSFC, China Excellent Young Scholars Program, under Grants 61722212, in part by the National Science Foundation of China, under Grants 61873212, 61702444, 61572506, in part by the Pioneer Hundred Talents Program of Chinese Academy of Sciences, China in part by the the West Light Foundation, China of The Chinese Academy of Sciences, under Grant 2018-XBQNXZ-B-008. The authors would like to thank all anonymous reviewers for their constructive advices.

References

- [1] Ambros V. The functions of animal microRNAs. *Nature* 2004;431(7006):350.
- [2] Bartel DP. MicroRNAs: genomics, biogenesis, mechanism, and function. *Cell* 2004;116(2):281–97.
- [3] Blenkiron C et al. MicroRNA expression profiling of human breast cancer identifies new markers of tumor subtype. *Genome Biol* 2007;8(10):R214.
- [4] Jiang L et al. Altered let-7 expression in Myasthenia gravis and let-7c mediated regulation of IL-10 by directly targeting IL-10 in Jurkat cells. *Int Immunopharmacol* 2012;14(2):217–23.
- [5] Padgett KA et al. Primary biliary cirrhosis is associated with altered hepatic microRNA expression. *J Autoimmun* 2009;32(3–4):246–53.
- [6] Shi H et al. Walking the interactome to identify human miRNA-disease associations through the functional link between miRNA targets and disease genes. *BMC Syst Biol* 2013;7(1):101.
- [7] Mørk S et al. Protein-driven inference of miRNA-disease associations. *Bioinformatics* 2013;30(3):392–7.
- [8] Yang Y et al. MiRGOFs: A GO-based functional similarity measure for miRNAs, with applications to the prediction of miRNA subcellular localization and miRNA-disease association. *Bioinformatics* 2018.
- [9] Chen X et al. BNPMDA: bipartite network projection for MiRNA-disease association prediction. *Bioinformatics* 2018;34(18):3178–86.
- [10] Ashburner M et al. Gene ontology: tool for the unification of biology. *Nat Genet* 2000;25(1):25.
- [11] Lipscomb CE. Medical subject headings (MeSH). *Bull Med Libr Assoc* 2000;88(3):265.
- [12] Li Y et al. HMDD v2. 0: a database for experimentally supported human microRNA and disease associations. *Nucleic Acids Res* 2013;42(D1):D1070–4.
- [13] Lan W et al. Predicting microRNA-disease associations based on improved microRNA and disease similarities. *IEEE/ACM Trans Comput Biol Bioinf* 2018;15(6):1774–82.
- [14] Wang L et al. LMTRDA: using logistic model tree to predict MiRNA-disease associations by fusing multi-source information of sequences and similarities. *PLoS Comput Biol* 2019;15(3):e1006865.
- [15] Huang Z et al. HMDD v3. 0: a database for experimentally supported human microRNA-disease associations. *Nucleic Acids Res* 2018;47(D1):D1013–7.

- [16] Yang Z et al. dbDEMC 2.0: updated database of differentially expressed miRNAs in human cancers. *Nucleic Acids Res* 2016;45(D1):D812–8.
- [17] Jiang Q et al. miR2Disease: a manually curated database for microRNA deregulation in human disease. *Nucleic Acids Res* 2008;37(suppl_1):D98–D104.
- [18] Griffiths-Jones S. miRBase: microRNA sequences and annotation. *Curr Protoc Hum Genet* 2010;29(1).
- [19] Kozomara A, Griffiths-Jones S. miRBase: annotating high confidence microRNAs using deep sequencing data. *Nucleic Acids Res* 2013;42(D1):D68–73.
- [20] Zhang Z et al. PMRD: plant microRNA database. *Nucleic Acids Res* 2009;38(suppl_1):D806–13.
- [21] Guo Z-H, Yi H-C, You Z-H. Construction and comprehensive analysis of a molecular association network via lncRNA–miRNA–disease–drug–protein graph. *Cells* 2019;8(8):866.
- [22] Wang D et al. Inferring the human microRNA functional similarity and functional network based on microRNA-associated diseases. *Bioinformatics* 2010;26(13):1644–50.
- [23] Peng J et al. A learning-based framework for miRNA-disease association prediction using neural networks. *bioRxiv* 2018:276048.
- [24] Chen X et al. EGBMMDA: extreme gradient boosting machine for miRNA-disease association prediction. *Cell Death Dis* 2018;9(1):3.
- [25] Chen X et al. Novel human miRNA-disease association inference based on random forest. *Mol Ther Nucleic Acids* 2018;13:568–79.
- [26] Pan X, Shen H-B. Learning distributed representations of RNA sequences and its application for predicting RNA-protein binding sites with a convolutional neural network. *Neurocomputing* 2018;305:51–8.
- [27] Grover A, Leskovec J. node2vec: Scalable feature learning for networks. in *Proceedings of the 22nd ACM SIGKDD international conference on Knowledge discovery and data mining*. 2016. ACM.
- [28] Hulka BS, Stark AT. Breast cancer: cause and prevention. *Lancet (London, England)* 1995;346(8979):883.
- [29] Iorio MV et al. MicroRNA gene expression deregulation in human breast cancer. *Cancer Res* 2005;65(16):7065–70.
- [30] O'Brien CA et al. A human colon cancer cell capable of initiating tumour growth in immunodeficient mice. *Nature* 2007;445(7123):106–10.
- [31] Bandres E et al. Epigenetic regulation of microRNA expression in colorectal cancer. *Int J Cancer* 2009;125(11):2737–43.
- [32] Nathwani BN, Kim H, Rappaport H. Malignant lymphoma, lymphoblastic. *Cancer* 1976;38(2):964–83.
- [33] Miao Y-R et al. lncRNASNP2: an updated database of functional SNPs and mutations in human and mouse lncRNAs. *Nucleic Acids Res* 2017;46(D1):D276–80.
- [34] Chou C-H et al. miRTarBase update 2018: a resource for experimentally validated microRNA-target interactions. *Nucleic Acids Res* 2017;46(D1):D296–302.
- [35] Chen G et al. lncRNADisease: a database for long-non-coding RNA-associated diseases. *Nucleic Acids Res* 2012;41(D1):D983–6.
- [36] Cheng L et al. lncRNA2Target v2. 0: a comprehensive database for target genes of lncRNAs in human and mouse. *Nucleic Acids Res* 2018;47(D1):D140–4.
- [37] Piñero J et al. DisGeNET: a comprehensive platform integrating information on human disease-associated genes and variants. *Nucleic Acids Res* 2016;p. gkw943.
- [38] Szklarczyk D et al. The STRING database in 2017: quality-controlled protein-protein association networks, made broadly accessible. *Nucleic Acids Res* 2016;p. gkw937.
- [39] Wishart DS et al. DrugBank 5.0: a major update to the DrugBank database for 2018. *Nucleic Acids Res* 2017;46(D1):D1074–82.
- [40] Davis AP et al. The comparative toxicogenomics database: Update 2019. *Nucleic Acids Res* 2018;47(D1):D948–54.
- [41] Chen X et al. HGIMDA: Heterogeneous graph inference for miRNA-disease association prediction. *Oncotarget* 2016;7(40):65257.
- [42] Yu D-L, Ma Y-L, Yu Z-G. Inferring microRNA-disease association by hybrid recommendation algorithm and unbalanced bi-random walk on heterogeneous network. *Sci Rep* 2019;9(1):2474.